



HAL
open science

An auto-adaptive heat transfer model predicting the temperature evolution in photobioreactors

Ali Gharib, Walid Djema, Francesca Casagli, Olivier Bernard

► **To cite this version:**

Ali Gharib, Walid Djema, Francesca Casagli, Olivier Bernard. An auto-adaptive heat transfer model predicting the temperature evolution in photobioreactors. 22nd IFAC World Congress, Jul 2023, Yokohama, Japan. pp.9715-9720, 10.1016/j.ifacol.2023.10.284 . hal-04390482

HAL Id: hal-04390482

<https://inria.hal.science/hal-04390482>

Submitted on 12 Jan 2024

HAL is a multi-disciplinary open access archive for the deposit and dissemination of scientific research documents, whether they are published or not. The documents may come from teaching and research institutions in France or abroad, or from public or private research centers.

L'archive ouverte pluridisciplinaire **HAL**, est destinée au dépôt et à la diffusion de documents scientifiques de niveau recherche, publiés ou non, émanant des établissements d'enseignement et de recherche français ou étrangers, des laboratoires publics ou privés.



Distributed under a Creative Commons Attribution 4.0 International License

An auto-adaptive heat transfer model predicting the temperature evolution in photobioreactors^{*}

A. Gharib^{*} W. Djema^{*} F. Casagli^{*} O. Bernard^{*}

^{*} Université Côte d’Azur (UCA), Inria, INRAE, CNRS, Sorbonne Université, Biocore Team, 06902 Sophia Antipolis—Valbonne, France.

ali.gharib@inria.fr, walid.djema@inria.fr,
francesca.casagli@inria.fr, olivier.bernard@inria.fr

Abstract: This work is a first step towards a generic and highly flexible dynamical heat transfer model for unravelling the complex nonlinear dynamics of microalgae growing in different cultivation systems and under different climates. Physical models for predicting reactor temperature are crucial to simulate a wide range of scenarios and therefore for applying a more efficient on-line system control, according to present and future weather conditions. However, adapting these models to different reactor designs is complex, since they require many parameters. In this work, a model predicting the temperature evolution in two pilot-scale outdoor reactors is developed, using weather measurements and records of temperature in the process. Firstly, we introduce the new model and demonstrate the identifiability of its parameters. Then, the model is calibrated and validated using experimental data from two different cultivation systems. The resulting model turns out to be flexible enough to predict temperature evolution in two different reactor configurations. The results show that the designed model is efficient to predict short/mid terms evolution, while it may require recalibration over longer time periods.

Keywords: Modelling, Temperature, Identifiability, Nonlinear, Dynamical systems, Microalgae.

1. INTRODUCTION

Microalgae are unicellular microorganisms with a great potential exploited in many biotechnological applications (*e.g.*, wastewater remediation and biofuel production [12, 13]). However, their growth dynamics are very complex, due to nonlinear interactions between physical and biological phenomena [11]. In particular, temperature has a great impact on microalgae growth rates and yields [17]. Consequently, outdoor reactors are highly sensitive to the constantly changing weather conditions. An accurate prediction of temperature dynamics in outdoor systems is then crucial to derive optimal strategies for maximizing microalgae productivity. Achieving a temperature dynamics modelling requires a reliable heat balance description.

Recently developed heat transfer models provide a high temperature prediction accuracy of open raceway ponds ([3, 6]), which are shallow outdoor paddle-wheel-agitated photobioreactors. However, these models require a deep knowledge of the specific cultivation system, its geometry, its technical specificity along with a wide set of physical parameters. Thus, adapting these very specific models to every reactor configuration is a hard and time consuming task.

In the literature, some simplified models have been already

^{*} This work has received funding from the Digitalgaesation project within the European Union’s Horizon 2020 research and innovation program under the Marie Skłodowska-Curie grant agreement No. 955520. It also benefited from the support of the ADEME Biomsa project.

proposed, see, *e.g.*, Alonso-Bastida *et al.* [1] where an auto-adaptive temperature prediction model dedicated to an indoor photobioreactor is developed, and Casagli *et al.* [8], where a linear auto regressive model for a specific outdoor reactor is proposed. However, these models are not flexible and cannot be easily adapted to different configurations. In our work, we introduce a versatile heat transfer model that has a simple structure relying on physical principles, achieving accurate predictions for outdoor applications, and which has the advantage of being manageable in different configurations by adapting its parameters. For that purpose, we start from the heat transfer model given in [6], which was validated over different seasons for predicting temperature in an algae-bacteria outdoor reactor (raceway pond). In our approach, a simpler and generic version of the model in [6] is developed, and the identifiability of the versatile reduced-model is investigated. Both experimental data and data generated through the mechanistic model in [6] are used to calibrate the designed model in two different configurations.

The paper is organized as follows. In Section 2, we firstly introduce the general structure of the model combining microalgae dynamics and temperature evolution. Then, we recall the model of temperature provided in [6], and we introduce the generic reduced-model. Then, in Section 3, we address the issues of identifiability and identification of the reduced-model. In Section 4, we illustrate the results and the behavior of the calibrated system. Finally, Section 5 concludes the paper.

2. THE MATHEMATICAL MODELS

2.1 The general model describing microalgae dynamics

The growth of microalgae depends on several physical inputs, including light intensity (I) and temperature (T). In this section, we consider a variant of the model proposed in [2] representing the dynamics of an algal biomass (x_m), taking into account the effect of T and I on the growth rate of microalgae. This model is described by,

$$\begin{cases} \dot{x}_m = \mu(I, T, x_m)x_m - \frac{q^{in}}{V}x_m, \\ \dot{T} = \mathcal{T}(T, T_a, I, q^{in}, \dots), \\ \dot{V} = \mathcal{V}(T, T_a, q^{in}, q^{out}, \dots), \end{cases} \quad (1)$$

where, μ is the growth rate of microalgae, q^{in} is the inflow rate of water, and V is the liquid volume in a raceway pond. The photosynthetic efficiency is also highly influenced by the culture depth, so the average growth rate is given by,

$$\bar{\mu}(I_0, T, x_m) = \frac{1}{L} \int_0^L \mu(I(z), T, x_m) dz, \quad (2)$$

where L is the maximum depth, I_0 the incident light at the pond's surface. The irradiance $I(z)$, at a depth z , is decreasing exponentially due to light attenuation in the culture. Thus, light distribution along the reactor is described by the Beer-Lambert Law,

$$I(z) = I_0 \exp(-\xi z), \quad z \in [0, L], \quad (3)$$

where ξ is the light attenuation parameter.

From (1)-(2), we highlight that predicting efficiently the temperature evolution T is crucial in any microalgae cultivation system. Thus, in the sequel, we focus on the physical processes involving the T and V -dynamics.

Firstly, in the next section, we recall the heat transfer model introduced in [6], predicting the dynamics of temperature and depth over a raceway pond.

2.2 The full-model of temperature

Béchet *et al.* introduced in [3] a heat flux model for raceway ponds, which has been recently extended and validated over one year experimental data by Casagli *et al.* in [6]. The model has three states and uses the data from observed weather data (air temperature T_a (K), light intensity I_0 (W m^{-2}), relative humidity RH (-), wind speed v_r (m s^{-2})), and the rain q^r ($\text{m}^3 \text{m}^{-2} \text{s}^{-1}$) as well as the inflow and outflow rate q^{in} and q^{out} ($\text{m}^3 \text{s}^{-1}$). The dynamics of the model described in [6] are governed by,

$$\rho_w C_{pw} \frac{d(VT_P)}{dt} = Q_{ra,p} + Q_{ra,s} + Q_{ra,a} + Q_{h,evap} + Q_{conv} + Q_{h,in} + Q_{h,out} + Q_{h,rain} - Q_{conv,cond_w,co}, \quad (4)$$

$$S \frac{dh_L}{dt} = -S \frac{m_e}{\rho_w} + q^r + q^{in} - q^{out}, \quad (5)$$

$$\rho_{co} V_{co} C_{p,co} \frac{dT_{co}}{dt} = Q_{conv,cond_w,co} + Q_{cond}, \quad (6)$$

where T_P (K) is the reactor temperature, ρ_w (kg m^{-3}) is the water density, C_{pw} ($\text{J kg}^{-1} \text{K}^{-1}$) is the specific heat capacity of the water, S (m^2) is the reactor surface and h_L

(m) the pond depth, $Q_{ra,p}$ (W) is the radiation from the reactor surface, $Q_{ra,s}$ (W) is the total (direct and diffuse) solar radiation, $Q_{ra,a}$ (W) is the radiation from the air to the water, $Q_{h,evap}$ (W) is the evaporation flux, Q_{conv} (W) is the convective flux at the water surface, $Q_{h,in}$ (W) (resp. $Q_{h,out}$) is the heat flux associated with the influent (resp. effluent) water and $Q_{h,rain}$ (W) is the heat flux related to rain.

The term $Q_{conv,cond_w,co}$ is the conductive/convective flow related to the heat exchange between water and concrete. The parameter $h_{w,co}$ ($\text{W m}^{-2} \text{K}^{-1}$) is the heat transfer coefficient between the water (w) and the reactor support (co), and T_{co} (K) is the temperature of the concrete.

Eq. (5) is the dynamics for the water level, where: m_e ($\text{kg s}^{-1} \text{m}^{-2}$) is the evaporation rate, respectively. Eq. (6) describes the temperature dynamics of the concrete support, where Q_{cond} is the conductive heat flux with the ground at the reactor bottom (W). We refer to [6] for further details on each transfer contribution ((4)-(6)).

The model described in [6] is complex, involving several parameters and requiring a deep knowledge of the system. However, for control purposes a simpler model is needed. The main objective is therefore to extract from (4)-(6) the structure of a generic heat transfer model, flexible enough to be adapted to any photobioreactor and which can be easily calibrated. In the following section, the procedure followed to reduce the model complexity is reported.

2.3 The reduced-model of temperature

Our aim is to design an accurate model involving less parameters. According to Bechet *et al.* [3] and to Casagli *et al.* [6], the most relevant terms in the heat balance are $Q_{ra,p}$, $Q_{ra,s}$, $Q_{ra,a}$, $Q_{h,evap}$, and Q_{conv} . Focusing only on these terms, and simplifying their expressions, results in a much simpler structure involving less parameters. On the other hand, numerical results show that the fluxes $Q_{h,rain}$, $Q_{conv,cond_w,co}$ and Q_{cond} have negligible effect on the predicted temperature. We also note that the $Q_{h,evap}$ term in (4) is slightly simplified in the reduced model, due to its high complexity. The influent flow rate q^{in} drives the process dynamics, and it is often the main control variable of the process. Similarly, the liquid depth can also be an efficient control variable to regulate temperature. These two variables q^{in} and q^{out} are maintained in the versatile reduced model since they will be used as control variables of the system. The resulting model is then given by,

$$\begin{aligned} \dot{T}_p(T_p, T_a, I_0, v_0, RH, q^{in}, \theta) = & (aA(T_p) + bB(T_p^4) + cC(T_a) \\ & + dD(T_a^4) + eE(I_0) \\ & + \alpha F(T_p, T_a, v_0, RH) \\ & + Q_{in}(T_p, q^{in})) / (\lambda_7 h S) \end{aligned} \quad (7a)$$

$$\begin{aligned} \dot{h}(T_p, T_a, q^{in}, q^{out}, q_{rain}, \theta) = & (\alpha F(T_p, T_a, v_0, RH)) / \lambda_8 \\ & + q^{in} / S - q^{out} / S + q_{rain} \end{aligned} \quad (7b)$$

with,

$$A(T_p) = \lambda_1 T_p \quad (7c)$$

$$B(T_p^4) = \lambda_2 T_p^4 \quad (7d)$$

$$C(T_a) = \lambda_3 T_a \quad (7e)$$

$$D(T_a^4) = \lambda_4 T_a^4 \quad (7f)$$

$$E(I_0) = \lambda_5 I_0 \quad (7g)$$

$$F(T_p, T_a, v_0, RH) = -\lambda_6 m_e \quad (7h)$$

$$m_e = v_0^{0.8} (P(T_p) - RH \times P(T_a))$$

$$P(\zeta) = \lambda_9 \exp(\lambda_{10} + \lambda_{11}(\zeta - \lambda_{12})^{0.5})/\zeta$$

$$Q_{in}(T_p, q^{in}) = \lambda_7 q^{in}(T_{in} - T_p) \quad (7i)$$

$$q^{out} = \frac{h(t)^{14}}{h(t)^{14} + h_{L,max}^{14}} \lambda_{13} \quad (7j)$$

where S is the surface of the reactor, λ_i are some known constants taken from [6], and $T_{in} = 20^\circ C$ is the temperature of the influent flow, which is assumed to be constant. The vector of parameters is then defined as,

$$\theta = [a, b, c, d, e, \alpha] \quad (8)$$

Notice that the reduced-model involves only six unknown parameters (the surface S is given) and two state variables, while the model in [6] involves up to 27 parameters.

3. MODEL IDENTIFICATION

3.1 Structural identifiability analysis

We consider a generic model with state x , inputs u , output y and parameterized by a vector θ :

$$\begin{aligned} \dot{x} &= f(x, u, \theta) \\ y &= g(x, u, \theta) \end{aligned} \quad (9)$$

The model (9) is said to be structurally identifiable [19] if $y(x(\theta_1), u, \theta_1) = y(x(\theta_2), u, \theta_2) \implies \theta_1 = \theta_2$. (10)

In our case, model (7) is linear with respect to its parameters. There are specific results for proving the identifiability of this class of systems [18] when the full state (here T_p and h) is supposed to be measured. The main result of [18] for Linear-in-Parameters Dynamical Systems can be extended for systems which are Linear-in-Parameters with combinations of the functions of the state and of functions of inputs. Assuming that the inputs (here the temperatures) are independent, the identifiability problem consists in determining if there is a unique solution to the equations given by N measurements of temperature T_p and of its derivative,

$$\begin{pmatrix} \dot{T}_p(t_1) \\ \dot{T}_p(t_2) \\ \vdots \\ \dot{T}_p(t_N) \end{pmatrix} = \mathcal{A}\theta + \begin{pmatrix} Q_{in}(t_1) \\ Q_{in}(t_2) \\ \vdots \\ Q_{in}(t_N) \end{pmatrix}, \quad (11)$$

where

$$\mathcal{A} = \begin{pmatrix} A(t_1) & B(t_1) & C(t_1) & D(t_1) & E(t_1) & F(t_1) \\ A(t_2) & B(t_2) & C(t_2) & D(t_2) & E(t_2) & F(t_2) \\ \vdots & \vdots & \vdots & \vdots & \vdots & \vdots \\ A(t_N) & B(t_N) & C(t_N) & D(t_N) & E(t_N) & F(t_N) \end{pmatrix} \quad (12)$$

The question is then the rank of \mathcal{A} for $N > 5$. Let us assume that there is a linear relationship between the functions of T_p , T_p^4 , $1/T_p$ and functions of independent inputs. This means,

$$A(T_p) + \rho_1 B(T_p) + \rho_2 C(T_a) + \rho_3 D(T_a) + \rho_4 E(I_0) + \rho_5 F(T_p, T_a) = 0, \quad (13)$$

after differentiating this constraint, we get,

$$\begin{aligned} \dot{T}_p \left(\frac{dA}{dT_p}(T_p) + \rho_1 \frac{dB}{dT_p}(T_p) + \rho_5 \frac{\partial F}{\partial T_p}(T_p, T_a) \right) \\ + \rho_2 \dot{T}_a \frac{dC}{dT_a}(T_a) + \rho_3 \dot{T}_a \frac{dD}{dT_a}(T_a) \\ + \rho_4 \dot{I}_0 \frac{dE}{dI_0}(I_0) + \rho_5 \dot{T}_a \frac{\partial F}{\partial T_a}(T_p, T_a) = 0 \end{aligned} \quad (14)$$

which is a differential equation describing the dynamics of T_p , independent from Eq. (7a), and which can not be simultaneously followed by T_p . Therefore \mathcal{A} is of full rank.

3.2 Practical identifiability analysis

Proving practical identifiability is a complementary task to structural identifiability that has to be addressed. Practical identifiability shows the uniqueness of solutions under the impact of experimental data (non noise-free data any more) [11]. The Fisher Information Matrix (FIM) is calculated by,

$$\text{FIM} = \sum_{i=1}^N \left[\frac{\partial y}{\partial \theta}(t_i) \right]^T \text{K} \left[\frac{\partial y}{\partial \theta}(t_i) \right], \quad (15)$$

where $\frac{\partial y}{\partial \theta} = (\sigma_T, \sigma_h)^T$ are the sensitivity functions, K the inverse of the measurement error covariance matrix. By obtaining,

$$V = \text{FIM}^{-1} = \left[\sum_{i=1}^N \left[\frac{\partial y}{\partial \theta}(t_i) \right]^T \text{K} \left[\frac{\partial y}{\partial \theta}(t_i) \right] \right]^{-1} \quad (16)$$

as the inverse of the FIM and the sensitivity functions of the output variables,

$$\frac{d}{dt} \left(\frac{\partial y}{\partial \theta} \right) = \begin{bmatrix} \dot{\sigma}_T \\ \dot{\sigma}_h \end{bmatrix} = \begin{bmatrix} \frac{\partial \dot{T}_p}{\partial T_p} & \frac{\partial \dot{T}_p}{\partial h} \\ \frac{\partial \dot{h}}{\partial T_p} & \frac{\partial \dot{h}}{\partial h} \end{bmatrix} \begin{bmatrix} \sigma_T \\ \sigma_h \end{bmatrix} + \begin{bmatrix} \frac{\partial \dot{T}_p}{\partial \theta} \\ \frac{\partial \dot{h}}{\partial \theta} \end{bmatrix} \quad (17)$$

the confidence intervals

$$\theta \pm t_{\alpha; N-p} \sqrt{V_{ii}} \quad (18)$$

are calculated with V_{ii} as the diagonal entries of V . The values of $t_{\alpha; N-p}$ are obtained from Student distributions [11].

Identification: Considering the dynamics of system (9) and the available measurements from the actual system output y_m sampled at time t_i :

$$y_m(t_i) = g(x(t_i), u, \theta^*) + \epsilon(t_i) \quad (19)$$

where ϵ is the measurement noise. The objective is to find the value of θ minimising the prediction error:

$$\bar{E}(\theta) = \sum_{i=1}^{N_H} (\delta(t_i, \theta))^2, \quad (20)$$

where,

$$\delta(t_i, \theta) = y(t_i, \theta) - y_m(t_i), \quad \text{for } i \in \{1, \dots, N_H\}. \quad (21)$$

The prediction error quantifies the performance of the model output along the sampling instants t_i (N_H is the number of measurements available for y).

The optimization problem is defined as,

$$\begin{aligned} \min_{\theta} \quad & \bar{E}(\theta) \\ \text{s. t.} \quad & \theta \in \Theta \end{aligned} \quad (22a)$$

where Θ denotes the parameter domain. Since the parameters are positive, we consider that,

$$\Theta = \{\theta : \theta_i \geq 0, \text{ for } i = 1, \dots, 6\}. \quad (23)$$

The optimization problem defined in Eq. (22a) aims to fit the parameters of the versatile reduced-model to either measured data, or simulated data from the full-model. The Levenberg-Marquardt algorithm [14, 15] is used through the lsqnonlin-toolbox in Matlab 2020b. In addition, in order to get a faster and more accurate convergence of the parameters, we compute the gradient of the error function,

$$\frac{\partial E}{\partial \theta} = \frac{\partial E}{\partial y} \frac{\partial y}{\partial \theta} \quad (24a)$$

$$\frac{d}{dt} \left(\frac{\partial y}{\partial \theta} \right) = \mathbb{J} \frac{\partial y}{\partial \theta} + \frac{\partial f}{\partial \theta} \quad (24b)$$

We also provide the analytic expressions of the sensitivity functions $\frac{\partial y}{\partial \theta}$ (see Eq. (17)) to the Matlab lsqnonlin function in order to compute the gradient $\frac{\partial E}{\partial \theta}$.

Computing the FIM: The FIM is calculated to check practical identifiability once a first guess of the parameters has been obtained. Then the procedure is iterated. The parameter set around which we want to obtain confidence intervals is the optimal parameter set,

$$\theta_{RM} = \begin{pmatrix} 0.9877 \\ 1.0157 \\ 1.0184 \\ 1.0219 \\ 0.7981 \\ 1.0928 \end{pmatrix} \quad (25)$$

obtained from the optimizing parameters of the versatile model to fit measured data (see Section 4.2).

Applying the calculations of Eq. (15) lead to

$$\text{FIM} = \sum_{i=1}^N \left[\frac{\partial y}{\partial \theta}(t_i) \right]^T \mathbf{K} \left[\frac{\partial y}{\partial \theta}(t_i) \right] = X^T \mathbf{K} X \quad (26)$$

where X are sensitivity functions. The value from Student distribution is $t_{\alpha; N-p} = 1.96$ for 95% (see [11]) and the confidence intervals result,

$$\begin{pmatrix} 0.7822 & 1.1932 \\ 0.8130 & 1.2184 \\ 0.7670 & 1.2697 \\ 0.7520 & 1.2919 \\ 0.5804 & 1.0158 \\ 0.8381 & 1.3475 \end{pmatrix} \quad (27)$$

for a data-set of four days (simulated data).

4. NUMERICAL RESULTS & SIMULATIONS

In this section we present the results of the versatile reduced-model prediction. For fitting the model to measured or simulated data (temperature and depth), we used a data-set of 200 points (approx. 4 days), starting from day 50. The initial parameter-set is $\theta_{init} = [1, 1, 1, 1, 1, 1]$.

4.1 Fitting towards the full-model

Firstly, we see how the model performs optimizing the fit with simulated data from the full-model. These simulated data are generated, by simulating a raceway located in Narbonne (France) using recorded weather data. The reactor is lying on the ground, has a surface $S = 56 \text{ m}^2$ and a total length of 15 m [6]. Fig. 1 shows that the error between the versatile reduced-model and the full-model is in a range of $[-0.57, 0.70]^\circ\text{C}$. The calibration data-set was in hotter days (day 50-54) and leads to a bigger error during colder days (days 200-270).

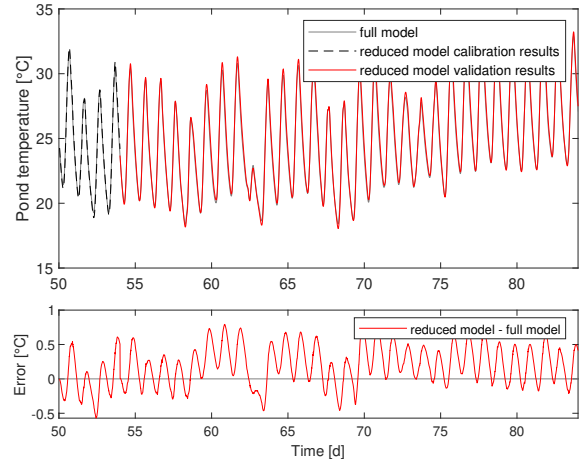


Fig. 1. Temperature dynamics of the full-model (grey line) and reduced-model (red line). A data-set of 4 days (200 points) is used to fit the simplified model to simulated data from the full-model [6].

4.2 Fitting towards measured data

The full-model in Eq. (4) was calibrated and validated using measured data from the same raceway as in Section 4.1. From the overall set of measured data composed of 10522 samples over 443 days, we use four days for identification (days 50-54). The absolute error δ is in a range of $[-1.1, 0.86]^\circ\text{C}$. Then, to validate the reduced-model, we use the remaining set of data (see Fig. 2). A 30 day prediction of the reduced-model with fitted parameters is represented by the continuous red line resulting in a deviation from the measured data of maximum $[-3.50, 2.81]^\circ\text{C}$.

It worth mentioning that even if the depth is not considered in the optimization objective (20), the model provides an accurate prediction of this variable, as illustrated in Fig. 3 where the maximum of the absolute error is small (0.024 m).

4.3 Performance comparison between the two models

This section presents a comparison between the full and reduced models. The parameters of the reduced-model are the ones optimized in Section 4.2. From the obtained results, we highlight that the reduced model provides accurate predictions (comparable to the ones given by the full-model, and even better in some cases) on short-and-mid time-horizons (see Fig. 4). However, the reduced-model is less efficient over longer-time periods, mainly due

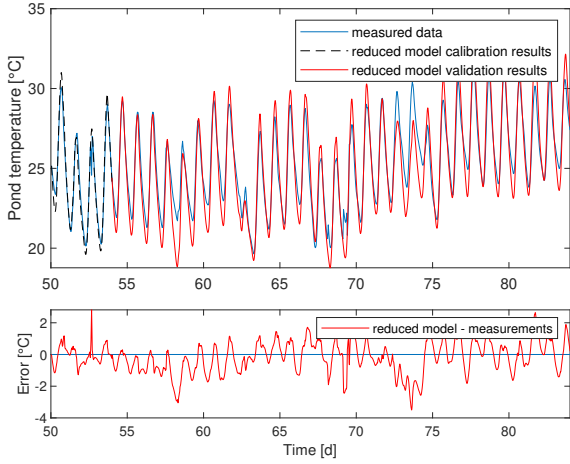


Fig. 2. Temperature dynamics of the measured data (blue line) and reduced-model (red line). A data-set of 4 days (200 points) is used to fit the reduced-model to measured data from the reactor in Narbonne.

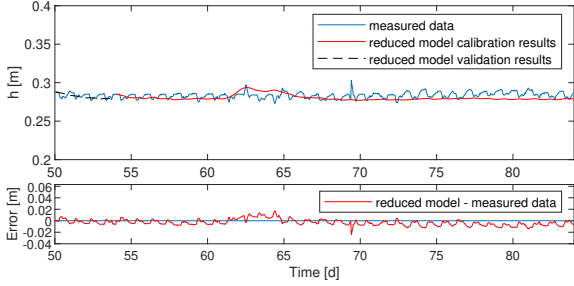


Fig. 3. Prediction of the depth associated with the data in Fig. 2.

to changing seasons (a re-calibration step is then needed). For instance, we observe in Fig. 4 that the prediction error is larger ($[-8.55, 7.76]^{\circ}\text{C}$) during the cold period (approximately between days 200 and 300) since it is far from the calibration range performed during summer.

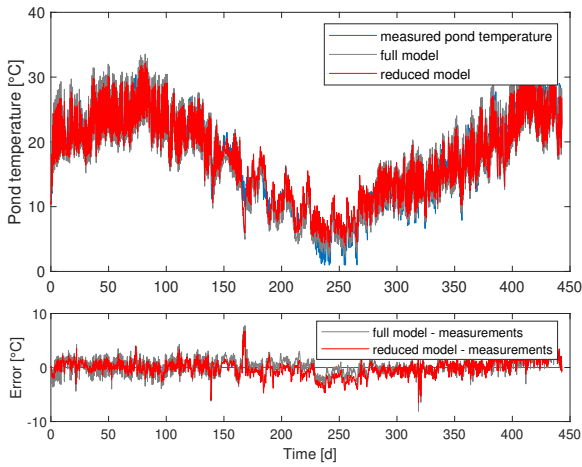


Fig. 4. Comparison of the temperature dynamics of the raceway in Narbonne: experimental data (blue line), reduced-model (red line) and full-model (grey line).

4.4 Accuracy as a function of the calibration window and prediction time horizon

Depending on the prediction horizon and on the time window selected for the identification phase, Fig. 5 shows how the deviation error evolves along the prediction time. Generally, the error increases with longer prediction time and smaller set of calibration data. The prediction error (σ_{SD}) is lower for a prediction time of approximately 100 days, using calibration-data for 4 or 9 days.

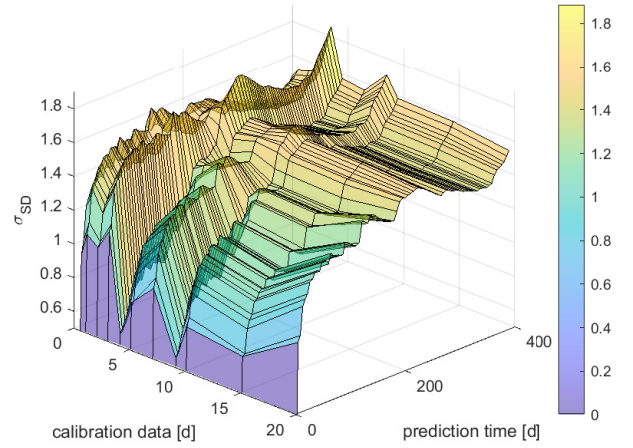


Fig. 5. Evolution of the error standard deviation σ_{SD} along the prediction, depending on the number of days used for calibration.

4.5 Validation on a different system

In this section, we evaluate the performance of the versatile reduced-model applied to a different data-set from a distinct geographical area (Milan, IT). These data are obtained from a raceway pond which is much smaller than the previous one (surface area of 3.8m^2) and raised from the ground. The volume (and so the depth) inside the reactor was kept constant during the operating period. For more details on the second reactor configuration we refer to [9, 16]. Fig. 6 shows that the prediction given by the reduced-model is very accurate along all the period, with a slightly overestimation observed on the highest temperature values. However, the average error obtained in this case is low (0.8875°C).

5. CONCLUSION

We designed a flexible model reacquiring a low number of parameters for describing the heat transfers and predicting the reactor temperature. The reduced-model was very accurate over short-and-mid term periods, while it needs recalibration for longer time-intervals. The next step will consist in using the developed model to design new control strategies for maintaining temperature in a desired domain, then optimizing the production of microalgae in different types of bioreactors ([5, 10, 4]).

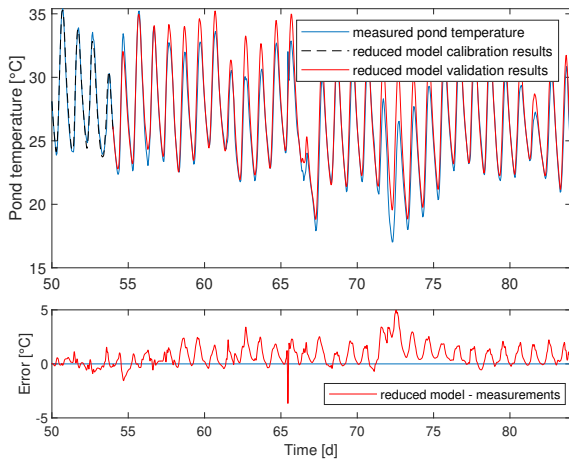


Fig. 6. Temperature dynamics of the measured data (blue line) and reduced-model (red line). Using a data-set of 4 days (200 points) to fit the reduced-model to measured data from the second reactor (Milan, IT).

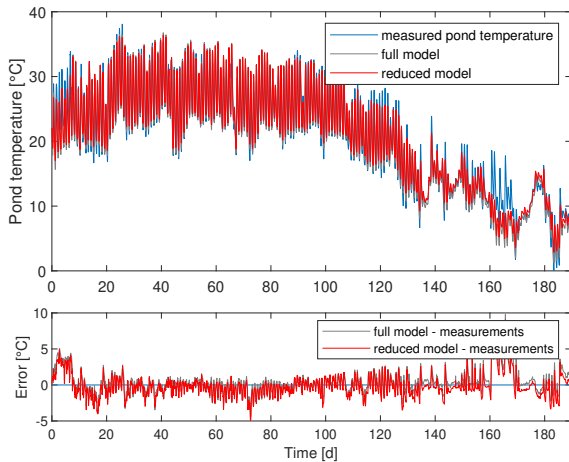


Fig. 7. Comparison of the temperature dynamics of the raceway in Milan: experimental data (blue line), reduced-model (red line) and full-model (grey line).

REFERENCES

- [1] Alonso-Bastida, A., Franco-Nava, M. A., Adam-Medina, M., López-Zapata, B., Álvarez-Gutiérrez, P. E., García-Morales, J., 2022. *Mathematical modeling of thermal interactions in a self-cooling pilot-scale photobioreactor* Case Studies in Thermal Engineering, 31, 101825.
- [2] Béchet, Q., Shilton, A., Guieysse, B., 2013. *Modeling the effects of light and temperature on algae growth: state of the art and critical assessment for productivity prediction during outdoor cultivation* Biotechnology advances, 31(8), 1648-1663.
- [3] Béchet, Q., Shilton, A., Park, J. B., Craggs, R. J., Guieysse, B., 2011. *Universal temperature model for shallow algal ponds provides improved accuracy.* Environmental science & technology.
- [4] Bernard, O., Mairet, F., Chachuat, B., 2015. *Modelling of microalgae culture systems with applications to control and optimization* Microalgae Biotechnology, 59-87.
- [5] Bernard, O. (2011). *Hurdles and challenges for modelling and control of microalgae for CO2 mitigation and biofuel production.* Journal of Process Control, 21(10), 1378-1389.
- [6] Casagli, F., Bernard, O., 2022. *Simulating biotechnological processes affected by meteorology: Application to algae-bacteria systems.* Journal of Cleaner Production, 377, 134190.
- [7] Casagli, F., Bernard, O. 2022. *How Heat Transfer Indirectly Affects Performance of Algae-Bacteria Raceways.* Microorganisms, 10(8), 1515.
- [8] Casagli, F., Rossi, S., Steyer, J. P., Bernard, O., Ficara, E., 2021. *Balancing microalgae and nitrifiers for wastewater treatment: can inorganic carbon limitation cause an environmental threat?* Environmental science & technology, 55(6), 3940-3955.
- [9] Casagli, F., Bernard, O., 2022. *Coupling heat transfer modelling to ALBA model for full predictions from meteorology* IFAC-PapersOnLine, 55(20), 558-563.
- [10] Djema, W., Bayen, T., Bernard, O., 2022. *Optimal Darwinian Selection of Microorganisms with Internal Storage Processes,* 10(3), 461.
- [11] Dochain, D., 2008. *Bioprocess control.* Academic Press., ISTE Ltd.
- [12] Jacob-Lopes, E., Maroneze, M.M., Queiroz, M.I. and Zepka, L.Q. eds., 2020. *Handbook of microalgae-based processes and products: fundamentals and advances in energy, food, feed, fertilizer, and bioactive compounds.* Academic Press.
- [13] Kumar, M., Sun, Y., Rathour, R., Pandey, A., Thakur, IS., Tsang, DCW., 2020, *Algae as potential feedstock for the production of biofuels and value-added products: Opportunities and challenges,* Science of the Total Environment, vol. 716, 137116.
- [14] Levenberg, K., 1944. *A Method for the Solution of Certain Problems in Least Squares* Quart. Appl. Math. Vol. 2.
- [15] Marquardt, D., 1963. *An Algorithm for Least-Squares Estimation of Nonlinear Parameters* SIAM J. Appl. Math. Vol. 11.
- [16] Pizzera, A., Scaglione, D., Bellucci, M., Marazzi, F., Mezzanotte, V., Parati, K., Ficara, E., 2019. *Digestate treatment with algae-bacteria consortia: A field pilot-scale experimentation in a sub-optimal climate area* Bioresource technology, 274, 232-243.
- [17] Ras, M., Steyer, JP., Bernard, O., 2013. *Temperature effect on microalgae: a crucial factor for outdoor production.* Reviews in Environmental science & Bio/Technology, 12(2), 153-164.
- [18] Stanhope, S., Rubin, J. E., Swigon, D., 2014. *Identifiability of linear and linear-in-parameters dynamical systems from a single trajectory* SIAM Journal on Applied Dynamical Systems, 13(4), 1792-1815.
- [19] Walter, E., Pronzato, L., 1997. *Identification of parametric models from experimental data.* Berlin, Springer.